

1        **Assessing the impact of climate variability and human activities**  
2                                **on streamflow variation**

3                                J. Chang, H. Zhang, Y. Wang, and Y. Zhu

4        State Key Laboratory Base of Eco-hydraulic Engineering in Arid Area, Xi'an University of  
5                                Technology, Xi'an 710048, China

6  
7        **ABSTRACT**

8        Water resources in river systems have been changing under the impact of both climate variability  
9        and human activities. Assessing the respective impact on decadal streamflow variation is important  
10       for water resource management. By using an elasticity-based method and calibrated TOPMODEL  
11       and VIC hydrological models, we quantitatively isolated the relative contributions that human  
12       activities and climate variability made to decadal streamflow changes in Jinghe basin, located in the  
13       northwest of China. This is an important watershed of Shaanxi Province that supplies drinking water  
14       for a population of over 6 million people. The results showed that the maximum value of the  
15       moisture index ( $E_0/P$ ) was 1.91 and appeared in 1991-2000, and the decreased speed of streamflow  
16       was higher since 1990 compared with 1960-1990. The average annual streamflow from 1990 to  
17       2010 was reduced by 26.96% compared with the multi-year average value (from 1960 to 2010). The  
18       estimates of the impacts of climate variability and human activities on streamflow decreases from  
19       the hydrological models were similar to those from the elasticity-based method. The maximum  
20       contribution value of human activities was 99% when averaged over the three methods, and was  
21       appeared in 1981–1990 due to the effects of soil and water conservation measures and irrigation  
22       water withdrawal. Climate variability made the greatest contribution to streamflow reduction in  
23       1991–2000, the values of which was 40.4%. We emphasized various source of errors and

24 uncertainties that may occur in the hydrological model (parameter and structural uncertainty) and  
25 elasticity-based method (model parameter) in climate change impact studies.

26 Keywords: Streamflow variation, Human activities, Climate variability, VIC model,  
27 TOPMODEL, Climate elasticity model

28

## 29 **1. Introduction**

30 Catchment hydrology and water resources are driven by climate and strongly  
31 modulated by human activities. Climate variability affects catchment streamflow,  
32 chiefly through precipitation and the variability of potential evaporation ([Scanlon et al.,](#)  
33 [2007](#); [Chien et al., 2013](#); [Ward et al., 2009](#); [Chang et al., 2010](#)). Human activities  
34 include land use/cover change, reservoir operations, and direct water extraction from  
35 surface-water and groundwater, all of which can alter river streamflow. It is important  
36 to separate and quantify the effects of climate variability and human activities so that  
37 they can be used for land use planning, water extraction and water resource  
38 management. With the increasing scarcity of water resources, hydrologists, decision  
39 makers and policy makers have paid considerable attention to how much of the  
40 observed change in annual streamflow can be attributed to climate variability and  
41 human activities ([Zhang et al., 2008](#); [Tomer and Schilling, 2009](#); [Roderick and](#)  
42 [Farquhar, 2011](#); [Destouni et al., 2013](#)).

43 Catchment experiments are very useful to determine the influence of vegetation  
44 change on the water balance; however, they are often limited to small scales. A number  
45 of catchment afforestation and deforestation studies have been conducted. Most of the  
46 results indicated that catchment streamflow significantly decreased after afforestation

47 and increased after deforestation (Van Lill et al., 1980; Zhang et al., 2001; Tuteja et al.,  
48 2007). Two other main approaches, process-based and statistic based, were generally  
49 used. The process-based method uses hydrological models to quantify the contribution  
50 of climate variability to streamflow change by varying the meteorological inputs for  
51 fixed land use/cover conditions (Xu et al., 2013; Petchprayoon et al., 2010; Lin et al.,  
52 2010; Tesfa et al., 2014; Zhang et al., 2012). Statistical methods for identifying the  
53 contributions of climate and human impacts on runoff were also used, especially in  
54 regions where long-term climate and hydrological data were available (Hamed, 2008;  
55 Notebaert et al.2011; Renner et al. 2012; Roudier et al. 2014). Among the statistical  
56 methods, streamflow elasticity was commonly used to quantify the influence of changes  
57 in precipitation and potential evapotranspiration on streamflow (Sankarasubramanian  
58 et al., 2001; Chiew, 2006; Fu et al., 2007; Roderick and Farquhar, 2011). Streamflow  
59 elasticity can be obtained non-parametrically from observations or by employing a  
60 parametric model, such as the Budyko hypothesis or other models. The Budyko  
61 hypothesis was widely used, as it was an easy method with a limited requirement for  
62 climate data (Donohue et al. 2007; Liu et al., 2009; Wang et al., 2011, 2013).

63 Climate change and human activities have had tremendous impact on the water  
64 resources of China's highly urbanized regions. One such river basin is the Jinghe River,  
65 which is the secondary tributary of the Yellow River, the largest tributary of the Weihe  
66 River in China, with an area of 45,400 km<sup>2</sup> and an average annual natural streamflow  
67 of 12.3×10<sup>8</sup> m<sup>3</sup>. This is an important watershed of Shaanxi Province that supplies  
68 drinking water for a population of over 6 million people. The area is an important

69 economic center of Shaanxi province in China, and the water shortage became a  
70 bottleneck for economic progress. Human activities, such as water withdrawal, soil and  
71 water conservation projects, have become extensive in the Jinghe River during the last  
72 several decades. Climate change studies in the Yellow River basin reported warming  
73 trends at a rate of 1.28 °C/50 years, while the average precipitation dropped by  
74 approximately 8.8% over the second half of the 20<sup>th</sup> century (Yang et al, 2004). A  
75 combination of these effects reduced the streamflow (Gao et al. 2013; Chang et al,  
76 2015). Few studies were devoted to use the methods of elasticity model together with  
77 hydrological model to quantitatively analyze the contributions of climate variability and  
78 human activities to streamflow variation in the Jinghe River basin.

79 The aims of this study were to: 1) present a generic framework that investigate the  
80 impact of climate variability and human activities on streamflow using the concept of  
81 streamflow elasticity and hydrological models, the TOPMODEL and VIC models,  
82 which are fundamentally different in regard to their representation of streamflow  
83 generation; and 2) compare these methods. The elasticity based method only provides  
84 results at a mean annual time scale, whereas the hydrological modeling results are at a monthly  
85 and daily scale, and they are aggregated to the mean annual time scale for comparison with  
86 those obtained from the statistical method.

87 The Jinghe River Basin (JRB) was chosen as the study area, which has presented a  
88 significantly decreasing trend of annual streamflow since 1990 (Chang et al, 2014; Du  
89 and Shi, 2012). This paper is organized as follows: Sect. 2 describes the study area and  
90 data sources; Sect.3 is devoted to introduce the methods used; Sect. 4 provides

91 hydrological modeling and the elasticity method results; Sect. 5 compares the results from  
92 the hydrological modeling with the elasticity-based method; and Sect. 6 discusses  
93 several conclusions generated from the present study.

## 94 **2. Study area and data**

95 The JRB (E106°14' ~ 108°42' , N34°46' ~ 37°19') is located in semiarid area in  
96 China and is approximately 455 km long, with a drainage area of 45400 km<sup>2</sup> (Fig. 1).  
97 The climate is temperate, with cool, dry winters and hot summers, and the mean annual  
98 temperature is in the 7.8-13.5 °C range across the basin. The mean annual precipitation  
99 is approximately 514 mm, 80% of which falls between June and October, and the mean  
100 annual potential evapotranspiration is 870 mm. The precipitation and streamflow both  
101 have strong inter-annual and intra-annual variabilities. The seasonal variation of  
102 streamflow is similar to that of precipitation. The streamflow between July and October  
103 is approximately 65% of the mean annual streamflow. Zhangjiashan station is the  
104 downstream hydrometric station on the main stream of the Jinghe River.

105 Human activities have become extensive in the JRB during the last several decades.  
106 Water withdrawal has increased rapidly due to the increase of the population, industry  
107 and agricultural water demand. Thick and highly erodible loess, unevenly distributed  
108 rainfall, and the relatively high intensity of rainstorms have led to high soil loss rates  
109 across the basin. To reduce soil loss, soil and water conservation measures have been  
110 undertaken since the 1970s, which have resulted in an increase in vegetation cover.  
111 Therefore, climate variability combined with human activities has contributed to the  
112 decrease of the streamflow in the JRB (Chang et al, 2014; Du and Shi, 2012).

113 **Fig. 1.** Location of hydrological and meteorological stations along the Jinghe  
114 River

115 In this study, the catchment information data set, including the catchment  
116 boundary and runoff ratio, was from the Ministry of Water Resources of the People's  
117 Republic of China. The daily, monthly, and annual climate variables and observed  
118 streamflow were used. The daily meteorological data, including precipitation, air  
119 temperature, sunshine hours, relative humidity, and wind speed, of ten stations during  
120 1960–2010 were collected from the China Meteorological Administration. The monthly  
121 and annual precipitation was then established from the collected data, and annual  
122 maximum, annual minimum, and multi-annual mean air temperature values were then  
123 calculated according to the daily data. The monthly potential evaporation was  
124 calculated according to the monthly wind speed, sunshine hours, relative humidity and  
125 air temperature using the Penman-Monteith method. The daily streamflow data of the  
126 Zhangjiashan hydrological station for the same period were gathered from the Shaanxi  
127 Hydrometric and Water Resource Bureau. The DEM data were obtained from the  
128 SRTM 30 m Digital Elevation Data. The soil data were extracted from the FAO two-  
129 layer 5-min 16-category global soil texture maps. Figure 1 also shows the location of  
130 the meteorological stations and hydrological station in the basin.

### 131 **3. Methodology**

#### 132 **3.1. Framework of Analysis**

133 The historic streamflow series can be split into two subseries according to the  
134 streamflow break year, and human activities in the recorded years prior to the break  
135 year can be negligible. The recorded years prior to this break year were defined as the

136 baseline period, while the recorded years after this break year were defined as the  
137 changed period. The difference between the mean annual streamflow during the  
138 changed period ( $Q_2$ ) and the mean annual streamflow during the baseline period ( $Q_1$ )  
139 represent the total change of the streamflow ( $\Delta Q$ ) after the break year. The  $\Delta Q$  can be  
140 regarded as a function of climatic variables and the integrated effects of topography,  
141 soil, land use/land cover and human activities, such as water withdrawing. Under the  
142 assumption that the topography and soil of the study area did not vary during the study  
143 period,  $\Delta Q$  was referred to as a combination of climate variability and human activities  
144 and can be estimated as the formulation:

$$\Delta Q = Q_2 - Q_1 \quad (1)$$

145 where  $\Delta Q$  is the total change in the mean annual streamflow and  $Q_1$  and  $Q_2$  are the  
146 average annual streamflows before and after an abrupt change, respectively.

148 The total change in the mean annual streamflow can be estimated as:

$$\Delta Q = \Delta Q_C + \Delta Q_H \quad (2)$$

149 where  $\Delta Q_C$  and  $\Delta Q_H$  are the changes in the mean annual streamflow due to climate  
150 and human activities, respectively.

### 152 3.2 Climate Elasticity Model for $\Delta Q_C$

153 The concept of streamflow elasticity was first introduced by [Schaake \(1990\)](#) to  
154 evaluate the sensitivity of streamflow to climate change. It represents the proportional  
155 change in streamflow divided by the proportional change in a climatic variable ( $X$ ),  
156 such as precipitation or potential evapotranspiration, and is expressed as:

$$\varepsilon = \frac{\partial Q/Q}{\partial X/X} \quad (3)$$

158 Thus, precipitation elasticity and evapotranspiration elasticity of streamflow were

159 defined by [Schaake \(1990\)](#) as:

$$160 \quad \varepsilon_P(P, Q) = \frac{dQ/Q}{dP/P} = \frac{dQ}{dP} \frac{P}{Q} \quad (4)$$

$$161 \quad \varepsilon_{E_0}(E_0, Q) = \frac{dQ/Q}{dE_0/E_0} = \frac{dQ}{dE_0} \frac{E_0}{Q} \quad (5)$$

162 where  $P$ ,  $E_0$  and  $Q$  are precipitation, potential evapotranspiration and streamflow,  
163 respectively.  $\varepsilon_P$  and  $\varepsilon_{E_0}$  are the elasticity of streamflow with respect to  $P$  and  $E_0$ ,  
164 respectively. Changes in these factors could lead to streamflow variation, and the  
165 relationship can be estimated as ([Milly and Dunne, 2002](#)):

$$166 \quad \Delta Q_C = (\varepsilon_P \Delta P/P + \varepsilon_{E_0} \Delta E_0/E_0)Q \quad (6)$$

167 where  $\Delta P$  and  $\Delta E_0$  are the changes in precipitation and potential evapotranspiration,  
168 respectively, and  $\varepsilon_P + \varepsilon_{E_0} = 1$ . To estimate  $\Delta Q_C$  using Eq. (6), the estimate of the  
169 precipitation elasticity of streamflow  $\varepsilon_P$  is needed. In this paper, the Budyko  
170 hypothesis was used to estimate  $\varepsilon_P$ .

171 The Budyko hypothesis ([Yang et al., 2008](#); [Teng et al., 2012](#); [Wang et al., 2015](#))  
172 produces a simplified, but powerful, coupled water-energy balance method. It is a  
173 holistic approach that assumes that water balance is controlled by water availability and  
174 atmospheric demand. The water availability can be approximated by precipitation. The  
175 atmospheric demand represents the maximum possible evapotranspiration and is often  
176 equated with potential evapotranspiration. The role of the landscape properties on the  
177 mean annual water balance is mainly implicit and is deemed to be subservient to the  
178 dominant role of climate. In some formulations of the Budyko formulation, the role of  
179 the landscape is represented by a separate, lumped parameter ([Yu et al., 2014](#); [Donohue](#)  
180 [et al., 2007](#)), which is nevertheless estimated empirically. According to the long-term



181 water balance equation ( $Q = P - E_a$ ) and the Budyko hypothesis, the actual  
 182 evapotranspiration ( $E_a$ ) is a function of the aridity index ( $\Phi = E_0/P$ ) and the precipitation  
 183 and potential evapotranspiration elasticity of streamflow can be expressed as (Arora,  
 184 2002; Dooge et al., 1999):

$$185 \quad \varepsilon_P = 1 + \Phi F'(\Phi)/(1 - F(\Phi)) \quad \text{and} \quad \varepsilon_P + \varepsilon_{E_0} = 1 \quad (7)$$

186 A couple of mathematical functions were proposed to represent the Budyko  
 187 hypothesis (e.g., Fu, 1996; Milly, 1993). We used the Budyko formulation of Fu (1981)  
 188 who combined a dimensional analysis with mathematical reasoning and developed  
 189 analytical solutions for the mean annual actual evapotranspiration:

$$190 \quad F(\Phi) = 1 + \Phi - (1 + \Phi^w)^{1/w} \quad (8)$$

191 where  $F(\Phi)$  is a function proposed by the Budyko, which not only satisfies the  
 192 boundary conditions under the land surface evapotranspiration but also remains  
 193 independent from the balance equation of hydrothermal coupling (the water balance  
 194 and energy balance).  $w$  is a model parameter with range  $(1, \infty)$ , which is related to  
 195 vegetation type, soil hydraulic property, and topography (Fu, 1996).  $w$  was set to  
 196 2.0, according to Li et al. (2013).

### 197 **3.3 Modeling-Based Approach for $\Delta Q_C$ or $\Delta Q_H$**

198 Hydrological models can also be used to assess the impact of climate change and  
 199 human activities on streamflow. A hydrological model was calibrated and validated to  
 200 estimate  $\Delta Q_C$  and  $\Delta Q_H$  by using the data from the baseline period. The model was run  
 201 using climate data (e.g., precipitation and temperature) during the changed period with  
 202 human activities (i.e., land use and management) and during the baseline period.  $\Delta Q_C$   
 203 was estimated as the difference between the mean annual average of simulated

204 streamflow during the changed period and the mean annual average of simulated  
205 streamflow during the baseline period.  $\Delta Q_H$  was estimated as the difference between  
206 the mean annual average of the simulated streamflow during the changed period and  
207 the mean annual average of the observed streamflow during the changed period.

208 In this study, two hydrological models, the TOPMODEL and VIC model, were used  
209 to investigate the effects of climate variability and human activities on streamflow.  
210 TOPMODEL (Beven and Kirkby, 1979) is a semi-distributed variable contributing area  
211 hydrological model. It is based on simple physical reasoning and assumes that there is  
212 a steady transfer of water in the saturated zone along hillslopes, with a water table nearly  
213 parallel to the ground surface. It considers two stream flow sources: (shallow)  
214 groundwater and saturation overland flow. The model assumes an exponential decay of  
215 soil transmissivity with increasing water table depth, and it considers two main  
216 parameters for the dynamics of the saturated store: the recession parameter  $m$  [L] and  
217 the average soil transmissivity at saturation  $T$  [ $LT^{-1}$ ]. The classical form for the  
218 topographic index that follows from the exponential assumption,  $\lambda_i = \ln(a/\tan b)$   
219 was used, where  $a$  is the drained area per unit length of the contour curve and  $b$  is  
220 the topographic gradient. All of the points in the catchment with the same topographic  
221 index were predicted as having the same deficit, i.e., they were considered to be  
222 hydrologically similar. The original TOPMODEL had four parameters: the maximum  
223 allowable root storage deficit ( $SR_{max}$ ), the transmissivity of the soil in the saturated state  
224 ( $T$ ), the maximum moisture max deficit ( $S_{zm}$ ), and the recharge delay parameter ( $T_d$ ).  
225 Since the early 1990s, TOPMODEL has widely been applied to watersheds all over the

226 world because it can provide spatially distributed hydrological information with  
227 available input requirements (e.g., Digital Elevation Model (DEM) data) (Seibert et al.,  
228 1997, Chen and Wu, 2012; Furusho et al., 2013). Some studies also applied  
229 TOPMODEL in semi-arid area basins, such as the Yellow River in China, and the  
230 results showed that this model was applicable over a wide range of environments  
231 (Xiong et al., 2004; Boston et al., 2004; Gumindoga et al., 2015).

232 The VIC model is a large-scale hydrological model that was originally developed  
233 at the University of Washington (Liang et al., 1994; Grimson et al, 2013; Gao et al.,  
234 2011). The hydrological processes of the model include the interaction of the  
235 atmosphere with underlying vegetation and soils, where dynamic water and energy  
236 fluxes are considered. One distinguishing characteristic of the VIC model is that it  
237 represents the sub-grid spatial heterogeneity of precipitation with the sub-grid spatial  
238 variability of soil infiltration capacity. A variable infiltration curve is used to represent  
239 the sub-grid variability of the soil infiltration capability under different land cover and  
240 soil types. Three types of potential evaporation are considered in the model: potential  
241 evaporation from the canopy layer of each vegetation class, transpiration from each of  
242 the vegetation classes, and bare soil potential evaporation. We used six parameters in  
243 the calibration of the VIC model. These included three baseflow parameters:  $D_m$ ,  $W_s$ ,  
244 and  $D_s$ ; the variable soil moisture capacity curve parameter:  $b$ ; and two parameters,  $d_2$   
245 and  $d_3$ , that controlled the thickness of the second and third soil layer, respectively. The  
246 VIC model was successfully applied to assess the impact of climate change on  
247 hydrology and water resources in China (Wang et al. 2010; Bao et al. 2012; Su and Xie,

248 2003; Liu et al. 2013).

249 We obtained the break points of precipitation and streamflow series in the JRB by  
250 means of a sequential cluster analysis method, and the break points appeared in 1968  
251 and 1970 respectively (Fig. 2), so we used 1960-1970 as the baseline period for this  
252 study. The TOPMODEL and VIC model were calibrated using the historical data from  
253 1960 to 1966 and validated against the observation during the period of 1967 to 1970.  
254 During the calibration, adjustments were made to minimize the sum of squares of the  
255 difference between the modeled and recorded monthly streamflow. Nash–Sutcliffe  
256 efficiency coefficients (NSE) and relative Water Balance Error percentage (WBE) were  
257 used for the model assessment using the observed data and model estimates.

$$258 \quad NSE = 1 - \frac{\sum_{i=1}^N (Q_{o,i} - Q_{s,i})^2}{\sum_{i=1}^N (Q_{o,i} - \overline{Q_o})^2} \quad (9)$$

$$259 \quad WBE = \left| \frac{100 * (\sum_{i=1}^N Q_{s,i} - \sum_{i=1}^N Q_{o,i})}{\sum_{i=1}^N Q_{o,i}} \right| \quad (10)$$

260 Where  $Q_{o,i}$  is the observed streamflow of period  $i$ ,  $Q_{s,i}$  is the simulated streamflow  
261 of period  $i$ , and  $\overline{Q_o}$  is the mean of observed streamflow.

262 **Fig. 2.** The abrupt change points of precipitation and streamflow in the JRB with Sequential cluster.

## 263 4. Results

### 264 4.1 The analysis of streamflow, precipitation, potential evaporation and 265 temperature

266 The regional average precipitation, potential evaporation and temperature in the  
267 JRB during 1960-2010 were calculated using the Thiessen polygon method of ArcGIS  
268 9.3, according to the corresponding data of ten hydrometeorology stations.

269 The annual observed precipitation in the JRB and streamflow at Zhangjiashan  
270 station both showed a statistically decreasing trend (Fig. 3), while the streamflow had

271 a larger decrease. The values of the regression slope were -1.44 and -0.58. The multi-  
272 year average streamflow (from 1960 to 2010) was 37.03 mm, and the average annual  
273 streamflow was 43.47 mm from 1960 to 1990, which meant that the streamflow from  
274 1960 to 1990 increased by 17.39% compared with the multi-year average streamflow.  
275 The average annual streamflow was 27.05 mm during 1991-2010 and was reduced by  
276 26.96% compared with the multi-year average value; therefore, the speed of the  
277 streamflow decrease was higher since 1990. The three-year moving curve showed that  
278 precipitation and streamflow fluctuation was similar, which indicated that precipitation  
279 was the main source of streamflow. The statistical results of precipitation, streamflow  
280 and the runoff coefficient in JRB are listed in Table 1. The maximums of precipitation  
281 and streamflow appeared at the same time in 1964; however, the minimum of  
282 precipitation and streamflow occurred in different years (1997 and 2009), which  
283 resulted from water withdrawal and other reasons, such as changes in groundwater. The  
284 precipitation and streamflow during the flood season (from July to October) accounted  
285 for 64.21% and 66.80%, respectively, and the proportion of the dry period (from  
286 November to March of next year) was 7.46% and 18.22%, respectively. The proportion  
287 of precipitation that became runoff was low, with a mean annual runoff ratio of 0.05,  
288 but increased during the wet years. The runoff ratios during the wet year and wet season  
289 were 0.08 and 0.06, respectively.

290 The result of Mann–Kendall’s test showed the same decreasing trend for the  
291 annual precipitation and streamflow in JRB from 1960 to 2010. The Z value of  
292 streamflow and precipitation was -4.26 (confidence level was 99%) and -1.39

293 (confidence level was 90%), respectively, which meant that the decreasing trend for  
294 streamflow was significant, but was insignificant for precipitation at a = 0.05 level.

295 **Fig. 3.** Changes of the annual streamflow and precipitation of the JRB.

296  
297 **Table1** Characteristics of the inter-annual streamflow and precipitation of the JRB.

298 Table 2 shows the monthly and seasonal potential evaporation and temperature in  
299 the JRB, which indicated that the potential evaporation (122 mm) and temperature  
300 (20.7 °C) in summer were much higher than the other three seasons, and the maximum  
301 values for the potential evaporation and temperature appeared in June and July,  
302 respectively. The inter-annual variation and characteristic values of the potential  
303 evaporation and temperature are shown in Fig. 4 and Table 3. The mean annual potential  
304 evaporation in the 1980s (822 mm) decreased compared with the values from the 1960s  
305 (861 mm) and started to increase slowly in the 1990s (973 mm). The temperature  
306 showed a slight upward trend in the 1970s and 1980s and had a sharp upward trend in  
307 the 1990s era. The Z values of potential evaporation and temperature for Mann–  
308 Kendall’s test were 0.4 and 4.12, respectively, which meant that the potential  
309 evaporation presented an insignificant increasing trend, but the temperature had a  
310 significant increasing trend.

311 **Table 2** The average monthly potential evaporation and temperature values of the JRB.

312  
313 **Table 3** Statistical values of the potential evaporation and temperature of the JRB.

314  
315 **Fig. 4.** Changes of the annual potential evaporation and temperature of the JRB.

## 316 317 **4.2 Climate Elasticity Model Results**

318 To assess the impact of climate variability on streamflow, the climate elasticity of  
319 streamflow was calculated using Eqs. (3) – (8) based on the annual precipitation and

320 annual potential evapotranspiration of the period from 1971 to 2010. Table 4  
321 summarizes the annual precipitation ( $P$ ), potential evapotranspiration ( $E_0$ ),  
322 precipitation elasticity ( $\varepsilon_P$ ), evapotranspiration elasticity ( $\varepsilon_{E_0}$ ) of streamflow for  
323 different periods, and percentage change in streamflow results for different periods  
324 when using the elasticity-based approaches. The variation of  $\varepsilon_P$  was between 1.45 and  
325 1.52, while the variation of  $\varepsilon_{E_0}$  was between -0.45 and -0.52. As shown in Table 4,  
326 for the period of 1971 to 2010, the values of  $\varepsilon_P$  and  $\varepsilon_{E_0}$  obtained were 1.48 and -0.48,  
327 respectively. The results indicated that a 10% decrease in precipitation would result in  
328 a 14.8% drop in streamflow, while a 10% decrease in potential evapotranspiration  
329 would induce a 4.8% increase of streamflow. According to Eq. (3), with the calculated  
330  $\varepsilon_P$  and  $\varepsilon_{E_0}$ , it was estimated that the 60.1 mm decrease in precipitation in 1971–2010  
331 might have decreased the streamflow by 40.9 mm; meanwhile, the 7.3 mm increase in  
332 the potential evapotranspiration may have caused a 5.1 mm decrease in streamflow.

333 The reductions in streamflow from 1971 to 2010 due to climate variability ranged  
334 between 7.5% and 29.9%, with a median of 19.3%, for the JRB when using the Budyko  
335 framework method. The maximum and minimum values of the moisture index ( $E_0/P$ ,  
336 Willmott, C.J. and Feddema, J.J., 1992) were 1.91 and 1.53, respectively, and appeared  
337 in 1991–2000 and 1981–1990, respectively. Compared with the 1960–1970 baseline  
338 period, the reductions in  $\Delta Q$  for 1991–2000 and 1981–1990 were  $5.7 \times 10^8 \text{ m}^3$  and  $4.0$   
339  $\times 10^8 \text{ m}^3$ , respectively, with climate variability making the greatest and smallest  
340 contributions (i.e., 29.9% and 7.5%, see Table 4).

341

342 **Table 4** The impact of climate variability and human activities on the streamflow with the

climate elasticity model.

### 4.3 Hydrological model calibration and validation

During the hydrological model simulation, the digital elevation quadrangles at a 30-m resolution in study area were used (Fig. 5). In TOPMODEL, several sub-basins were delineated according to the flow accumulation by means of ArcGIS, and the flow direction, flow accumulation were extracted in ArcGIS to calculate the topographic index-area ratio of sub-basin. The monthly precipitation, potential evapotranspiration and observed streamflow acted as the input data. Figure 6 shows the simulated and recorded streamflow for the calibration and validation periods. A calibrated VIC model was also employed to separate the hydrological impacts of land use change and climate change. The VIC model was used for the streamflow simulation at a 0.5 spatial and daily temporal resolution in the JRB (Fig. 5). Figure 6 shows the simulated and observed streamflows for the calibration and validation periods, with outputs computed on a monthly basis.

**Fig. 5.** (a) Elevation maps of the study area at a 30-m resolution. (b) Grid of the VIC model. (c) Sub-basin of TOPMODEL.

**Fig. 6.** The simulated and observed streamflow for TOPMODEL and the VIC model.

(a) Calibration period. (b) Validation period.

In the scatter plots in Fig. 7, the observed monthly streamflow was plotted along the  $x$  axis, and the model simulated streamflows (calibration and validation) were plotted along the  $y$  axis. The scatter plots in Fig. 7 showed that both the hydrological models performed reasonably well in the model calibration with high NSE values and low WBE values. The correlation of the simulated streamflow and measured streamflow ( $R$ ) was higher during the calibration period compared with the validation



369 period. The observed and simulated streamflow over the non-calibration period were  
370 compared to determine the suitability of the model for this study. The NSE, WBE and  
371  $R$  of TOPMODEL are 0.79, 2.1% and 0.987 in the calibration period, and are  
372 respectively 0.78, 9.2% and 0.944 in the validation period. The NSE, WBE and  $R$  of  
373 VIC model are 0.77, 3.5% and 0.944 in the calibration period, and are respectively 0.83,  
374 4.7% and 0.940 in the validation period. The NSE, WBE and  $R$  values during the  
375 validation period (see Fig. 7) suggested that both the rainfall–runoff models and the  
376 calibration method used in this study were robust for the calibrated model to be used  
377 over an independent simulation period adequately. Additionally, the results justified the  
378 suitability of the models applied for assessing the change in streamflow due to climate  
379 variability and human activities.

380 **Fig. 7.** Comparison of the observed and modeled monthly streamflows for the calibration and  
381 validation periods.

#### 382 **4.4 Hydrological model simulation results**

383 The calibrated model parameters for both the models from the baseline periods of  
384 1960 to 1970 were used with the meteorological time series to simulate the streamflow  
385 for the changed period of 1971 to 2010 and to investigate the effects of climate  
386 variability and human activities. The scatter plots in Fig. 8 and Fig. 9 show the  
387 comparison of the simulated and observed monthly and annual streamflow time series  
388 for the JRB for the entire modeling period (1971–2010) for TOPMODEL and the VIC  
389 model, respectively.

390 The model simulation results showed that streamflow had a strong response to the  
391 environmental change after 1970. In the scatter plots in Fig. 8, the simulated monthly

392 streamflow values are mostly above the 1:1 line, indicating that the simulated  
393 streamflow was much higher than the observed streamflow for most of the months. The  
394 number of the years that the simulated streamflow was higher than the observed  
395 streamflow was 26 from 1970 to 2010 for TOPMODEL, and the number was 25 for  
396 VIC model. Additionally, most of the years appeared before 1990 or after 2005 for both  
397 of the models, and in the rest of the years the simulated streamflow was similar or lower  
398 to the observed value. The effect of climate variability was eliminated from the  
399 simulations for the changed periods by using the actual observed climate to drive the  
400 calibrated models. The difference in the observed and simulated streamflows during the  
401 changed period was due to the difference in land cover and other human activities. The  
402 results indicated that human activities caused significant reductions in streamflow, and  
403 these results were consistent with other studies ([Chang et al., 2014](#); [Tang et al., 2013](#);  
404 [Zhan et al., 2014](#)).

405 **Fig. 8.** Comparison of the observed and modeled monthly streamflow in 1971-2010.

406 (a)TOPMODEL. (b) VIC model.

407

408 **Fig. 9.** Time series of the observed and modeled annual streamflow for the entire modeling period.

#### 409 **4.5 Influence of human activities and climate variability.**

410 To separate and quantify the effects of human activities on streamflow after 1970,  
411 the simulated streamflows for the two models were compared against the observed  
412 values during the baseline and changed periods (methodology details in Sect. 3.1). The  
413 differences in the observed streamflow values during the baseline and changed periods  
414 were caused by the differences in climatic conditions and human activities. Tables 5  
415 and 6 summarize the mean annual statistics of the observed and simulated streamflow

416 for the different periods of the 1970s, 1980s 1990s and 2000s. The third column  
417 provides the values for  $\Delta Q$ , which were the differences between the observed  
418 streamflow ( $Q_B$ ) during the changed periods and the baseline. The fourth column shows  
419 the simulated streamflow ( $Q_S$ ) for the changed periods when using climate and  
420 calibrated parameter values from the baseline period.  $\Delta Q_H$  was the difference between  
421  $Q_B$  and  $Q_S$  for the changed periods, and  $\Delta Q_C$  was the difference between  $Q_S$  for the  
422 changed period and  $Q_B$  of the baseline.  $\eta_C$  and  $\eta_H$  were the contribution ratios of  
423 climate change and human activities to streamflow, respectively.

424

425 **Table 5** The impact of climate variability and human activities on the streamflow with TOPMODEL.

426 **Table 6** The impact of climate variability and human activities on the streamflow with the VIC  
427 model.

428 The results showed that the average annual streamflow for 1971-2010 ( $12.3 \times 10^8$   
429  $\text{m}^3$ ) was less than that of the baseline period ( $18.3 \times 10^8 \text{ m}^3$ ), which meant that the  
430 recorded streamflow in the JRB markedly decreased over the past few decades. The  
431 total reduction  $\Delta Q$  in streamflow for the changed period of 1971 to 2010 (compared  
432 to the baseline period) due to human activities and climate variability for the JRB were  
433  $4.6 \times 10^8 \text{ m}^3$  and  $1.4 \times 10^8 \text{ m}^3$  for the TOPMODEL, which was approximately 76.7% and  
434 23.3% of the total reduction, respectively. The corresponding reductions were  $4.7 \times 10^8$   
435  $\text{m}^3$  (78.3%) and  $1.3 \times 10^8 \text{ m}^3$  (21.7%) for the VIC model.

436 For the different periods of 1970s, 1980s, 1990s and 2000s, the reductions in  
437 streamflow due to human activities were  $5.6 \times 10^8 \text{ m}^3$  (81.2% of the total change),  $3.8$   
438  $\times 10^8 \text{ m}^3$  (95% of the total change),  $3.0 \times 10^8 \text{ m}^3$  (52.6% of the total change) and  $6.1 \times 10^8$   
439  $\text{m}^3$  (82.4% of the total change) for TOPMODEL model, respectively. For the VIC

440 model, the reductions in streamflow due to human activities for the 1970s, 1980s, 1990s  
441 and 2000s were and  $5.7 \times 10^8 \text{ m}^3$  (82.6% of the total change),  $4.5 \times 10^8 \text{ m}^3$  (112.5% of the  
442 total change),  $3.2 \times 10^8 \text{ m}^3$  (56.1% of the total change) and  $5.8 \times 10^8 \text{ m}^3$  (78.4% of the  
443 total change), respectively. Compared to the baseline period of 1960 to 1970,  
444 streamflow greatly decreased during 2001–2010. The change impacts (i.e.,  $\Delta Q_H$  and  
445  $\Delta Q_C$ ) in 2001–2010 were approximately 77.4% ( $\Delta Q_H$ ) and 22.6% ( $\Delta Q_C$ ) of the total  
446 reduction when averaged over the two methods.

## 447 **5. Discussion**

### 448 **5.1 Results of comparing the three methods**

449 We used elasticity-based analyses, TOPMODEL and the VIC model, to isolate the  
450 hydrological impact of human activities from that of climate variability. The climate  
451 elasticity method is relatively simple and can easily be transplanted to other areas, and  
452 it provides a general streamflow change with less data and parameters (Ma et al. (2010)).  
453 On the contrary, the hydrological modeling method more precisely distinguishes the  
454 streamflow change, such as the monthly change or daily change. In this paper, the three  
455 methods were implemented independently at different time scales (climate elasticity  
456 method based on the yearly scale, TOPMODEL based on the monthly scale and VIC  
457 model hydrological simulation based on the daily scale (Peng D. Z., and Xu, Z. X.  
458 2010)). For the whole JRB, the contribution ratios of climate variability in 1971-2010  
459 were 23.3%, 21.7% and 19.3% from TOPMODEL, the VIC hydrological modeling  
460 method and the elasticity method, respectively, and the mean contribution ratio was  
461 21.4%. The most significant climate variability impacts were  $2.7 \times 10^8 \text{ m}^3$  (47.4%),  
462  $2.5 \times 10^8 \text{ m}^3$  (43.9%) and  $1.7 \times 10^8 \text{ m}^3$  (29.9%) for TOMODEL, the VIC model and the

463 elasticity based model, respectively, appearing in the 1990s. The most significant  
464 human activities impacts were  $3.8 \times 10^8 \text{ m}^3$  (95%),  $4.5 \times 10^8 \text{ m}^3$  (112.5%) and  $3.7 \times 10^8$   
465  $\text{m}^3$  (92.4%) for TOMODEL, the VIC model and the elasticity based model, respectively,  
466 appearing in the 1980s. The analysis showed that the results from the two hydrological  
467 models were similar to those from the commonly used elasticity-based approach.  
468 Additionally, the results of the three methods showed that the significant climate  
469 variability impacts appeared in the 1990s, and the significant human activities impacts  
470 appeared in the 1980s. The precipitation and temperature are the dominant factors of  
471 climate changes, and it is shown that the maximum decrease of precipitation appeared  
472 in the 1990s compared with baseline period (1960s), and the minimum decrease was in  
473 the 1980s (table 7). The temperature showed a significant increase in the 1990s, but an  
474 insignificant increase in the 1980s. The changes of precipitation and temperature for  
475 different decades verified that the significant climate variability impacts appeared in  
476 the 1990s. We concluded that the three methods were in good agreement in terms of  
477 the dominant contributor, i.e., human activities played a more important role in the  
478 streamflow decrease than the change in climate in the JRB. The main result of this  
479 research agreed with the findings of other studies in Northwest China. [Tang et al. \(2013\)](#)  
480 used the climate elasticity method and the Soil and Water Assessment Tool (SWAT)  
481 model to evaluate the impact of climate variability on streamflow in the Yellow River  
482 basin, This two methods gave consistent results. [Zhan et al. \(2014\)](#) developed an  
483 improved climate elasticity method based on the original climate elasticity method and  
484 conducted a quantitative assessment of the impact of climate change and human

485 activities on the streamflow decrease in the Wei River basin. The results from the  
486 improved climate elasticity method yielded a climatic contribution to the streamflow  
487 decrease of 22-29% and a human contribution of 71-78%.

488 **Table 7** Changes of the inter-annual precipitation and temperature of the JRB.

489 There are still differences in terms of the magnitude of each attributor. Compared to  
490 the results of the hydrological model, TOPMODEL and VIC model, the streamflow  
491 variation caused by climate variability estimated from the elasticity-based methods was  
492 smaller and that caused by human activities was larger, which agreed with the results  
493 of [Li et al. \(2012\)](#) and [Sun et al. \(2014\)](#). Except for the annual precipitation change,  
494 which was the most important factor in the streamflow change, the inter-annual and  
495 intra-annual precipitation variability, as second order climate effects, could lead to a  
496 significant change in streamflow. However, these second order climate effects cannot  
497 be taken into account in the elasticity-based methods, while they can be considered in  
498 the dynamic hydrological modeling method, which may partially explain the difference  
499 in the results ([Potter and Chiew, 2011](#)).

## 500 **5.2. Errors and uncertainties with each approach**

501 The elasticity-based assessment of environmental change on streamflow has more  
502 advantages than the hydrological modeling approach because it does not require  
503 detailed spatial input data. In this paper, the elasticity coefficient (i.e., the sensitivity  
504 coefficient of streamflow to climatic variable changes) was estimated. While it was  
505 commonly suggested that catchment properties were spatially and temporally varied  
506 and were influential on the streamflow of the watershed ([Roderick and Farquhar, 2011](#);  
507 [Donohue et al., 2011](#)), the errors from both the model structure (Budyko equations) and

508 the model parameter in Fu's model ( $w$ ), which we assumed to be temporally consistent,  
509 caused the elasticity-based analysis to not be error-free.

510 For the hydrological model of TOPMODEL and the VIC model, due to the errors of  
511 the model structure, input time series, and initial and boundary conditions, the  
512 predictions of physically based distributed models commonly contained a certain  
513 degree of uncertainty. For example, the higher resolution of the DEM (digital elevation  
514 model), the smaller input time series scale and the optimal model parameters would  
515 obtain better simulated results.

### 516 **5.3 The cause for streamflow change**

517 The results indicated that human activities were the dominant factors (approximately  
518 80%) for the streamflow decrease in 1971–2010 in the study area. There were several  
519 types of human activities that influenced streamflow, including water conservancy  
520 projects, large hydraulic projects, and water withdrawal for industry and agricultural  
521 demand. The human-induced reduction in streamflow in the JRB was primarily caused  
522 by soil and water conservation measures and water withdrawal (Shi, 2013; Zhao, 2013).

523 From Table 8, it can be observed that the large-scale soil conservation area expanded  
524 with time to prevent soil and water loss since the 1970s. As shown in Table 8, the  
525 amount of afforestation and level terrace land steadily increased since 1970 and that the  
526 amount of grass-planting land markedly increased since 1990. As of the 2000s, newly  
527 increased soil and water conservation areas in the basin were composed of 2907 km<sup>2</sup> of  
528 terrace land, 4773 km<sup>2</sup> of afforestation land, 1146 km<sup>2</sup> of grassland and 52 km<sup>2</sup> of  
529 dammed land. These soil conservation practices intercept precipitation, change local

530 characteristics, improve the infiltration rate of water flow, slow down or retain the  
531 streamflow, and consequently delay or even reduce streamflow. Additionally, during  
532 the past few decades, there were dramatic increases in the population and the irrigated  
533 area in the study area, which could have resulted in increased water withdrawal from  
534 the river. The evaluation of the individual effects on the hydrological regime still poses  
535 a challenge for hydrologists.

536

537 **Table 8** Cumulative area of soil and water conservation in JRB at the end of different years  
538 (Unit:km<sup>2</sup>).

539

## 540 **6. Conclusion**

541 This paper investigated the impact of human activities and climate variability on  
542 streamflow using observed data and three methods (an elasticity-based method, a  
543 calibrated TOPMODEL and VIC model) for the JRB in China.

544 (1) The variability of streamflow, precipitation, potential evaporation and  
545 temperature in the JRB was analyzed. The annual precipitation and streamflow both  
546 showed a statistically decreasing trend, while the streamflow had a larger decrease, and  
547 the decrease in speed was higher since 1990. The potential evaporation presented an  
548 insignificant increasing trend; however, the temperature had a significant increasing  
549 trend.

550 (2) The precipitation elasticity ( $\varepsilon_P$ ) and evapotranspiration elasticity ( $\varepsilon_{E0}$ ) of  
551 streamflow for different periods were calculated using the Budyko formulation of Fu.  
552 The results indicated that a 10% decrease in precipitation would result in a 14.8%  
553 drop in streamflow, while a 10% decrease in potential evapotranspiration would



554 induce a 4.8% increase of streamflow.

555 (3) Compared to the baseline period of 1960 to 1970, streamflow in the JRB  
556 greatly decreased during 2001–2010. Climate variability and human activities impacts  
557 from the hydrological models were similar to those from the elasticity-based method.

558 (4) The maximum contribution value of human activities appeared in 1981-1990  
559 due to the effects of soil and water conservation measures and water withdrawal for  
560 industry and agricultural water demand, whereas climate variability made the greatest  
561 contributions to the streamflow reduction in 1991–2000. The contribution ratios of  
562 human activities and climate variability were 99% and 40.4% when averaged over the  
563 three methods.

564

## 565 **Acknowledgments**

566 This research was supported by the Natural Science Foundation of China (51190093)  
567 and Key Innovation Group of Science and Technology of Shaanxi (2012KCT-10).  
568 Sincere gratitude is extended to the editor and the anonymous reviewers for their  
569 professional comments and corrections.

570

571

572

## 573 **References**

574 Arora, V.K.: The use of the aridity index to assess climate change effect on annual runoff, *J. Hydrol.*,  
575 265, 164–177, 2002.

576 Bao, Z., Zhang, J., Wang, G., Fu, G., He, R., Yan, X., Jin, J., Liu, Y., and Zhang, A.: Attribution  
577 for decreasing streamflow of the Haihe River basin, northern China: Climate variability or

578 human activities, *J. Hydrol.*, 460–461, 117–129, [doi.org/10.1016/j.jhydrol.2012.06.054](https://doi.org/10.1016/j.jhydrol.2012.06.054), 2012.

579 Beven, K.J., and Kirkby, M.J.: A physically based variable contributing area model of basin  
580 hydrology, *Hydrological Sciences Bulletin*, 24, 43-69 1979.

581 Boston, T., Xia, J., and Zhu, Y.: Pre-processing rainfall data from multiple gauges to improve  
582 TOPMODEL simulation results in a large semi-arid region, *Hydrol. Process.*, 18, 2313–2325,  
583 [doi:10.1002/hyp.5530](https://doi.org/10.1002/hyp.5530), 2004.

584 Chang, F.-J., Chang, L.-C., Kao, H.-S., and Wu, G.-R.: Assessing the effort of meteorological  
585 variables for evaporation estimation by self-organizing map neural network, *J. Hydrol.*, 384,  
586 118-129, 2010.

587 Chang, J.-X., Wang, Y., Istanbuluoglu, E., Bai, T., Huang, Q., Yang, D., and Huang, S.: Impact  
588 of climate change and human activities on runoff in the Weihe River Basin, China, *Quatern.  
589 Int.*, **380-381**, 169-179, 2015.

590 Chen, J. and Wu, Y.: Advancing representation of hydrologic processes in the Soil and Water  
591 Assessment Tool (SWAT) through integration of the TOPographic MODEL (TOPMODEL)  
592 features, *J. Hydrol.*, 420–421, 319–328, [doi:10.1016/j.jhydrol.2011.12.022](https://doi.org/10.1016/j.jhydrol.2011.12.022), 2012.

593 Chien, H., Yeh, P. J.-F., and Knouft, J. H.: Modeling the potential impacts of climate change on  
594 streamflow in agricultural watersheds of the Midwestern United States, *J. Hydrol.*, 491, 73–88,  
595 [doi:10.1016/j.jhydrol.2013.03.026](https://doi.org/10.1016/j.jhydrol.2013.03.026), 2013.

596 Chiew, F.H.S.: Estimation of rainfall elasticity of streamflow in Australia, *Hydrologic Science  
597 Journal* 51, 613–625, 2006.

598 Destouni G, Jaramillo F, and Prieto C.: Hydroclimatic shifts driven by human water use for food  
599 and energy production, *Nat Clim Change* 3, 213-217, [doi.org/10.1038/nclimate1719](https://doi.org/10.1038/nclimate1719), 2013.

600 Donohue, R.J., Roderick, M.L., and McVicar, T.R.: On the importance of including vegetation  
601 dynamics in Budyko's hydrological model, *Hydro. Earth Syst. Sci.*, 11, 983–995, [doi:](https://doi.org/10.5194/hess-11-983-2007)  
602 [10.5194/hess-11-983-2007](https://doi.org/10.5194/hess-11-983-2007), 2007.

603 Donohue, R.J., Roderick, M.L., and McVicar, T.R.: Assessing the differences in sensitivities of  
604 runoff to changes in climatic conditions across a large basin, *J. Hydrol.*, 406, 234–244,  
605 [doi.org/10.1016/j.jhydrol.2011.07.003](https://doi.org/10.1016/j.jhydrol.2011.07.003), 2011.

606 Dooge, J.C., Bruen, M., and Parmentier, B.: A simple model for estimating the sensitivity of  
607 runoff to long-term changes in precipitation without a change in vegetation, *Adv. Water*  
608 *Resour.*, 23, 153–163, 1999.

609 Du J., and Shi C.: Effects of climate factors and human activities on runoff of the Weihe River in  
610 recent decades. *Quaternary International*. 282, 58-65, 2012

611 Fu, B.P.: On the calculation of the evaporation from land surface, *Chinese Journal of Atmospheric*  
612 *Sciences*, 5, 23–31, 1981.

613 Fu, B.P.: On the calculation of evaporation from land surface in mountainous areas, *Scientia*  
614 *Meteorologica Sinica* 6, 328– 335, 1996.

615 Fu, G., Charles, S.P., and Chiew, F.S.H.: A two-parameter climate elasticity of streamflow index  
616 to assess climate change effects on annual streamflow, *Water Resour. Res.* 43, W11419.  
617 [doi:10.1029/2007WR005890](https://doi.org/10.1029/2007WR005890), 2007.

618 Furusho, C., Chancibault, K., and Andrieu, H.: Adapting the coupled hydrological model ISBA-  
619 TOPMODEL to the long-term hydrological cycles of suburban rivers: evaluation and sensitivity  
620 analysis, *J. Hydrol.*, 485, 139–147, 2013.

621 Gao, H., Bohn, T.J., Podest, E., McDonald, K.C., and Lettenmaier, D.P.: On the causes of the

622 shrinking of lake Chad, *Environ. Res. Lett.* 6, 034021, [doi:10.1088/1748-9326/6/3/034021](https://doi.org/10.1088/1748-9326/6/3/034021),

623 2011.

624 Gao, P., Geissen, V., Ritsema, C. J., Mu, X.-M., and Wang, F.: Impact of climate change and

625 anthropogenic activities on stream flow and sediment discharge in the Wei River basin, China,

626 *Hydrol. Earth Syst. Sci.*, 17, 961–972, [doi:10.5194/hess-17-961-2013](https://doi.org/10.5194/hess-17-961-2013), 2013.

627 Grimson, R., Montroull, N., Saurral, R., Vasquez, P., and Camilloni, I.: Hydrological modelling of

628 the Iber á Wetlands in southeastern South America, *J. Hydrol.*, 503, 47–54,

629 [doi:10.1016/j.jhydrol.2013.08.042](https://doi.org/10.1016/j.jhydrol.2013.08.042), 2013.

630 Gumindoga, W., Rientjes, T. H. M., Haile, A. T., and Dube, T.: Predicting streamflow for land

631 cover changes in the Upper Gilgel Abay River Basin, Ethiopia: a TOPMODEL based approach,

632 *Phys. Chem. Earth*, 76-78, 3-15, 2014.

633 Hamed, K.H.: Trend detection in hydrologic data: the Mann–Kendall trend test under the scaling

634 hypothesis, *J. Hydro.* 349, 350–363, 2008.

635 Li, D., Pan, M, Cong, Z., and Wood, E.: Vegetation control on water and energy balance within

636 the Budyko framework, *Water Resour. Res.* 49, 969-976, [doi: 10. 1002/wrcr.20107](https://doi.org/10.1002/wrcr.20107), 2013.

637 Li, H., Zhang, Y., Vaze, J., and Wang, B.: Separating effects of vegetation change and climate

638 variability using hydrological modelling and sensitivity-based approaches, *J. Hydro.*, 420–421,

639 403–418, 2012.

640 Liang, X., Lettenmaier, D.P., Wood, E.F., and Burges, S.J.: A simple hydrologically based model

641 of land surface water and energy fluxes for GSMs, *J. Geophys. Res.* 99, 415–428, 1994.

642 Lin, S.-H., Liu, C.-M., Huang, W.-C., Lin, S.-S., Yen, T.-H., Wang, H.-R., Kuo, J.-T., and Lee, Y.

643 C.: Developing a yearly warning index to assess the climatic impact on the water resources of

644 Taiwan, a complex-terrain island, *J. Hydrol.*, 390, 13–22, 2010.

645 Liu, H., Tian, F.\*, Hu, H. C., Hu, H. P., and Sivapalan, M.: Soil moisture controls on patterns of  
646 grass green-up in Inner Mongolia: an index based approach, *Hydrol. Earth Syst. Sci.*, 2013,  
647 17:805-815, doi:10.5194/hess-17-805-2013.

648 Liu, Q., Yang, Z., Cui, B., and Sun, T.: Temporal trends of hydro-climatic variables and runoff  
649 response to climatic variability and vegetation changes in the Yiluo River basin, China, *Hydro.*  
650 *Process.*, 23, 3030–3039, 2009.

651 Ma H, Yang D, Tan SK, Gao B, and Fu Q.: Impact of climate variability and human activity on  
652 streamflow decrease in the Miyun Reservoir catchment, *J. Hydro.*, 389: 317-324, 2010.

653 Milly, P.C.D.: An analytic solution of the stochastic storage problem applicable to soil water,  
654 *Water Resource Res.*, 29, 3755– 3758, 1993.

655 Milly, P.C.D., and Dunne, K.A.: Macroscale water fluxes 2. Water and energy supply control of  
656 their inter-annual variability, *Water Resour. Res.*, 38, 241–249, 2002.

657 Notebaert, B., Verstraeten, G., Ward, P., Renssen, H., and Van Rompaey, A.: Modeling the  
658 sensitivity of sediment and water runoff dynamics to Holocene climate and land use changes at  
659 the catchment scale, *Geomorphology* 126, 18–31, 2011.

660 Petchprayoon, P., Blanken, P.D., Ekkawatpanit, C., and Hussein, K.: Hydrological impacts of  
661 land use/land cover change in a large river basin in central–northern Thailand, *Int. J. Climatol.*,  
662 30, 1917–1930, 2010.

663 Peng D. Z., and Xu, Z. X.: Simulating the impact of climate change on streamflow in the Tarim  
664 River basin by using a modified semi-distributed monthly water balance model. *Hydrol.*  
665 *Process.* 24, 209–216 (DOI: 10.1002/hyp.7485). 2010.

666 Potter, N.J., and Chiew, F.H.S.: An investigation into changes in climate characteristics causing  
667 the recent very low runoff in the southern Murray– Darling Basin using rainfall–runoff models,  
668 Water Resour. Res., 47, [doi.org/10.1029/2010WR010333](https://doi.org/10.1029/2010WR010333), 2011.

669 Renner M, Seppelt R, and Bernhofer C: Evaluation of water-energy balance frameworks to predict  
670 the sensitivity of streamflow to climate change. Hydrol. Earth Syst. Sci., 16, 1419-1433, [doi:](https://doi.org/10.5194/hess-16-1419-2012)  
671 [10.5194/hess-16-1419-2012](https://doi.org/10.5194/hess-16-1419-2012), 2012.

672 Roderick, M.L., and Farquhar, G.D.: A simple framework for relating variations in runoff to  
673 variations in climatic conditions and catchment properties, Water Resour. Res., 47, W00G07,  
674 [doi: 10.1029/2010WR009826](https://doi.org/10.1029/2010WR009826), 2011.

675 Roudier, P., Ducharne, A., and Feyen, L.: Climate change impacts on runoff in West Africa: a  
676 review. Hydrol. Earth Syst. Sci., 18, 2789-2801, [doi: 10.5194/hess-18-2789-2014](https://doi.org/10.5194/hess-18-2789-2014), 2014.

677 Sankarasubramanian, A., Vogel, R.M., Limbrunner, J.F.: Climate elasticity of streamflow in the  
678 United States, Water Resour. Res., 37, 1771–1781, 2001.

679 Scanlon, B.R., Jolly, I., Sophocleous, M., and Zhang, L.: Global impacts of conversion from  
680 natural to agricultural ecosystem on water resources: quantity versus quality, Water Resour.  
681 Res., 43, W03437. [dx.doi.org/10.1029/2006WR005486](https://dx.doi.org/10.1029/2006WR005486), 2007.

682 Schaake, J.C.: From climate to flow. In: Waggoner, P.E. (Ed.), Climate Change and U.S. Water  
683 Resources, John Wiley, New York, pp. 177–206, 1990.

684 Seibert, J., Bishop, K.H., and Nyberg, L.: A test of TOPMODEL’s ability to predict spatially  
685 distributed groundwater levels, Hydrol. Process. 11, 1131–1144, 1997.

686 Shi C, Zhou Y, Fan X, et al. A study on the annual runoff change and its relationship with water  
687 and soil conservation practices and climate change in the middle Yellow River basin. Catena,

688 100: 31-41, 2013.

689 Su, F., and Xie, Z.: A model for assessing effects of climate change on runoff of China, *Prog. Nat.*  
690 *Sci.*, 13, 701–707, 2003.

691 Sun, Y., Tian, F., Yang, L., and Hu, H.: Exploring the spatial variability of contributions from  
692 climate variation and change in catchment properties to streamflow decrease in a mesoscale  
693 basin by three different methods, *J. Hydrol.*, 508, 170–180, 2014.

694 Tang, Y., Tang, Q., Tian, F., Zhang, Z., and Liu, G.: Responses of natural runoff to recent climatic  
695 variations in the Yellow River basin, China, *Hydrol. Earth Syst. Sci.*, 17, 4471–4480, doi:  
696 [10.5194/hess-17-4471-2013](https://doi.org/10.5194/hess-17-4471-2013), 2013.

697 Teng, J., Vaze, J., Chiew, F.H.S., Wang, B., and Perraud, J.M.: 2012. Estimating the relative  
698 uncertainties sourced from GCMs and hydrological models in modelling climate change impact  
699 on runoff, *J. Hydrometeorol.*, 13, 122–139, 2012.

700 Tesfa T.K., Li H.-Y., Leung, L. R. Huang, M., Ke, Y., Sun, Y., and Liu, Y.: A Subbasin-based  
701 framework to represent land surface processes in an Earth System Model, *Geosci. Model*  
702 *Dev.*, 7, 947-963, doi: [10.5194/gmd-7-947-2014](https://doi.org/10.5194/gmd-7-947-2014), 2014.

703 Tomer MD, and Schilling K.E.: A simple approach to distinguish land-use and climate-change  
704 effects on watershed hydrology, *J. Hydrol.*, 376: 24-33, 2009.

705 Tuteja, N.K., Vaze, J., Teng, J., and Mutendeudzi, M.: Partitioning the effects of pine plantations  
706 and climate variability on runoff from a large catchment in southeastern Australia, *Water*  
707 *Resour. Res.*, doi: [10.1029/2006WR005016](https://doi.org/10.1029/2006WR005016), 2007.

708 Van Lill, W.S., Kruger, F.J., and Van Wyk, D.B.: The effect of afforestation with Eucalyptus  
709 Grandis Hill ex Maiden and Pinus Patula Schlecht. et Cham. On streamflow from experimental

710 catchments at Mokobulaan, Transvaal, *J. Hydrol.*, 48, 107–118, 1980.

711 Wang, D., and Hejazi, M.: Quantifying the relative contribution of the climate and direct human  
712 impacts on mean annual streamflow in the contiguous United States, *Water Resour. Res.*, 47,  
713 W00J12, [doi.org/10.1029/2001wr000760](https://doi.org/10.1029/2001wr000760), 2011.

714 Wang, D., Hagen, S. C., and Alizad, K.: Climate change impact and uncertainty analysis of  
715 extreme rainfall events in the Apalachicola River basin, Florida, *J. Hydrol.*, 480, 125–135,  
716 2013.

717 Wang, D.B., Zhao, J.S., Tang, Y., and Sivapalan, M.: A thermodynamic interpretation of Budyko  
718 and L’vovich formulations of annual water balance: Proportionality Hypothesis and maximum  
719 entropy production, *Water Resour. Res.*, 51, 3007-3016, [doi: 10.1002/2014WR016857](https://doi.org/10.1002/2014WR016857), 2015

720 Wang, J.H., Hong, Y., Gourley, J., Adhikari, P., Li, L., and Su, F.G.: Quantitative assessment of  
721 climate change and human impacts on long-term hydrologic response: a case study in a sub-  
722 basin of the Yellow River. China, *Int. J. Climatol.*, 30, 2130–2137, [doi.org/10.1002/joc.2023](https://doi.org/10.1002/joc.2023),  
723 2010.

724 Ward, P.J., van Balen, R.T., Verstraeten, G., Renssen, H., and Vandenberghe, J.: The impact of  
725 land use and climate change on late Holocene and future suspended sediment yield of the  
726 Meuse catchment, *Geomorphology*, 103, 389–400, 2009.

727 Willmott, C.J., Robeson, S.M., and Feddema, J.J.: Influence of spatially variable instrument  
728 networks on climatic averages. *Geophysical Research Letters*, 18, 2249-2251, 1991.

729 Willmott, C.J. and Feddema, J.J.: A more rational climatic moisture index. *Professional*  
730 *Geographer*, 44, 84-88. [doi:10.1111/j.0033-0124.1992.00084](https://doi.org/10.1111/j.0033-0124.1992.00084). 1992.

731 Xiong, L. and Guo, S.: Effects of the catchment runoff coefficient on the performance of



732 TOPMODEL in rainfall–runoff modelling, *Hydrol. Process.*, 8, 1823–1836,  
733 [doi:10.1002/hyp.1449](https://doi.org/10.1002/hyp.1449), 2004.

734 Xu, X., Yang, H., Yang, D., and Ma, H.: Assessing the impacts of climate variability and human  
735 activities on annual runoff in the Luan River Basin, China, *Hydrol. Res.*, 44, 940–952,  
736 [doi.org/10.2166/nh.2013.144](https://doi.org/10.2166/nh.2013.144), 2013.

737 Yang D., Li C., Hu H., et al. Analysis of water resources variability in the Yellow River of China  
738 during the last half century using historical data[J]. *Water Resources Research*, 2004, 40(6).

739 Yang, H., Yang, D., Lei, Z., and Sun, F., New analytical derivation of the mean annual water-  
740 energy balance equation, *Water Resour. Res.*, 44, W034103, [doi: 10.1029/2007WR006135](https://doi.org/10.1029/2007WR006135),  
741 2008.

742 Yu Sun, Fuqiang Tian, Long Yang, Heping Hu. Exploring the spatial variability of contributions  
743 from climate variation and change in catchment properties to streamflow decrease in a mesoscale  
744 basin by three different methods. *J. Hydrol.*, 508,170–180, 2014.

745 Zhao, G., Mu, X., Tian, P., Wang, F., Gao, P., Climate changes and their impacts on water  
746 resources in semiarid regions: a case study of the Wei River basin, China. *Hydrol. Process.* 27,  
747 3852-3863, 2013.

748 Zhan, C. S., Jiang, S. S., Sun, F. B., Jia, Y. W., Niu, C. W., and Yue, W. F.: Quantitative contribution  
749 of climate change and human activities to runoff changes in the Wei River basin, China, *Hydrol.*  
750 *Earth System Sci.*, 18, 3069-3077, [doi: 10.5194/hess-18-3069-2014](https://doi.org/10.5194/hess-18-3069-2014), 2014.

751 Zhang, C., Peng, Y., Chu, J., Shoemaker, C. A., and Zhang, A.: Integrated hydrological modelling  
752 of small- and medium-sized water storages with application to the upper Fengman Reservoir  
753 Basin of China, *Hydrol. Earth Syst. Sci.*, 16, 4033–4047, [doi:10.5194/hess-16-4033-2012](https://doi.org/10.5194/hess-16-4033-2012), 2012.

754 Zhang, L., Dawes, W.R., and Walker, G.R.: Response of mean annual evapotranspiration to

755 vegetation changes at catchment scale, *Water Resour. Res.*, 37, 701–708, 2001.

756 Zhang, X., Zhang, L., Zhao, J., Rustomji, P., and Hairsine, P.: Responses of streamflow to

757 changes in climate and land use/cover in the Loess Plateau, China, *Water Resour. Res.*, 44,

758 W00A07, doi: [10.1029/2007WR006711](https://doi.org/10.1029/2007WR006711), 2008.

759

760

761

762

763

764

765

766

767

768

769

770

771

772

773

774

775

776

777

778

779

780

781

782

783 **Table 1** Characteristics of the inter-annual streamflow and precipitation of the JRB.

Feature	Mean (mm)	Maximum		Minimum		Extremes ratio	Variation coefficient $C_v$	Wet year (mm)	Flood period (%)	Dry period (%)
		time	(mm)	time	(mm)					
Precipitation	514	1964	794	1997	343	2.31	0.20	613.11	64.21	7.46
Streamflow	29.51	1964	85.46	2009	7.09	12.05	0.48	66.80	66.8	18.22
Runoff coefficient	0.05	1964	0.12	2009	0.04	3.34	0.28	0.08	—	—
Flood runoff coefficient	0.06	1964	0.12	2007	0.03	3.86	0.33	—	—	—

784

785

786

787

788

789

790

791

792

793

794

795

796

797

798

799

800

801

802

803

804

805

806  
807  
808  
809  
810  
811  
812  
813  
814  
815  
816  
817  
818

**Table 2** The average monthly estimated potential evaporation and temperature value of the JRB from 1960 to 2010.

Month	3	4	5	6	7	8	9	10	11	12	1	2
$E_0$ (mm)	61	90	118	131	126	108	70	49	32	24	26	34
Mean (mm)	90 (Spring)			122 (Summer)			50 (Autumn)			28 (Winter)		
$T$ (°C)	4.1	10.7	15.8	20	21.8	20.3	15.2	9.2	2.4	-3.3	-4.7	-1.7
Mean (°C)	10.2			20.7			8.9			-3.3		

821 Note:  $E_0$  was the potential evaporation;  $T$  was the temperature.

822  
823  
824  
825  
826  
827  
828  
829  
830  
831  
832  
833  
834  
835  
836  
837  
838  
839  
840  
841  
842  
843

844  
845  
846  
847  
848  
849  
850  
851  
852  
853  
854  
855  
856  
857  
858  
859  
860  
861  
862  
863  
864  
865  
866  
867  
868  
869  
870  
871  
872  
873  
874  
875  
876  
877  
878  
879  
880  
881  
882  
883

**Table 3** Statistical values of the potential evaporation and temperature of the JRB from 1960 to 2010.

Feature	Mean	$C_v$	$C_s$	Maximum		Minimum	
				time	Max	time	Min
$E_0$ (mm)	870	0.08	0.53	2004	1092	1964	713
$T$ (°C)	9.1	0.07	0.09	1998	10.2	1967	7.6

Note: the Mean was the multi-year average value;  $C_v$  was the deviation coefficient;  $C_s$  was the skewness coefficient;

884  
885  
886  
887  
888  
889  
890  
891  
892

**Table 4** The impact of climate variability and human activities on streamflow with the climate elasticity model.

Period	E <sub>0</sub> (mm)	P (mm)	Q (10 <sup>8</sup> m <sup>3</sup> )	aridity index	ΔE <sub>0</sub> (mm)	ΔP (mm)	ΔQ (10 <sup>8</sup> m <sup>3</sup> )	ε <sub>P</sub>	ε <sub>E0</sub>	ΔQ <sub>P</sub> (mm)	ΔQ <sub>E0</sub> (mm)	ΔQ <sub>C</sub> (mm)	Human activities		Climate variation		
													ΔQ <sub>H</sub> (10 <sup>8</sup> m <sup>3</sup> )	η <sub>H</sub> (%)	ΔQ <sub>C</sub> (10 <sup>8</sup> m <sup>3</sup> )	η <sub>C</sub> (%)	
1960-1970	846.5	561.2	18.3	1.54	—	—	—	—	—	—	—	—	—	—	—	—	—
1971-1980	894	500.1	11.4	1.79	29.5	-61.1	-6.9	1.46	-0.46	-40.6	-3.2	-43.9	-5.8	83.6	-1.1	16	
1981-1990	817.2	535.5	14.3	1.53	-47.3	-25.6	-4	1.49	-0.49	-18	6.3	-11.8	-3.7	92.4	-0.3	7.5	
1991-2000	881.9	462.4	12.6	1.91	17.5	-98.8	-5.7	1.45	-0.45	-64.2	-1.8	-66	-4	70.1	-1.7	29.9	
2001-2010	893.9	506.5	10.9	1.76	29.4	-54.6	-7.4	1.52	-0.52	-36.5	-3.3	-39.8	-6.4	86.1	-1	13.5	
1971-2010	871.8	501.1	12.3	1.74	7.3	-60.1	-6	1.48	-0.48	-40.9	5.1	-35.8	-4.8	80.7	-1.2	19.3	

893  
894  
895  
896  
897  
898  
899  
900  
901  
902  
903  
904  
905  
906  
907  
908  
909  
910  
911  
912  
913  
914  
915  
916  
917

918  
919  
920  
921  
922  
923  
924  
925

**Table 5** The impact of climate variability and human activities on streamflow with TOPMODEL.

Period	Annual mean streamflow			Human activities		Climate variation	
	$Q_B$ ( $10^8 \text{ m}^3$ )	$\Delta Q$ ( $10^8 \text{ m}^3$ )	$Q_S$ ( $10^8 \text{ m}^3$ )	$\Delta Q_H$ ( $10^8 \text{ m}^3$ )	$\eta_H$ (%)	$\Delta Q_C$ ( $10^8 \text{ m}^3$ )	$\eta_C$ (%)
1960-1970	18.3						
1971-1980	11.4	-6.9	17.0	-5.6	81.2	-1.3	18.8
1981-1990	14.3	-4.0	18.1	-3.8	95	-0.2	5
1991-2000	12.6	-5.7	15.6	-3.0	52.6	-2.7	47.4
2001-2010	10.9	-7.4	17.0	-6.1	82.4	-1.3	17.6
1971-2010	12.3	-6.0	16.9	-4.6	76.7	-1.4	23.3

926  
927  
928  
929  
930  
931  
932  
933  
934  
935  
936  
937  
938  
939  
940  
941  
942  
943  
944

945  
 946  
 947  
 948  
 949  
 950  
 951  
 952  
 953  
 954  
 955  
 956  
 957  
 958  
 959  
 960  
 961  
 962  
 963  
 964  
 965  
 966  
 967  
 968  
 969  
 970  
 971  
 972  
 973  
 974  
 975

**Table 6** The impact of climate variability and human activities on streamflow with the VIC model.

Period	Annual mean streamflow			Human activities		Climate variation	
	Q <sub>B</sub> (10 <sup>8</sup> m <sup>3</sup> )	ΔQ (10 <sup>8</sup> m <sup>3</sup> )	Q <sub>S</sub> (10 <sup>8</sup> m <sup>3</sup> )	ΔQ <sub>H</sub> (10 <sup>8</sup> m <sup>3</sup> )	η <sub>H</sub> (%)	ΔQ <sub>C</sub> (10 <sup>8</sup> m <sup>3</sup> )	η <sub>C</sub> (%)
1960-1970	18.3	—	—	—	—	—	—
1971-1980	11.4	-6.9	17.1	-5.7	82.6	-1.2	17.4
1981-1990	14.3	-4.0	18.8	-4.5	112.5	0.5	-12.5
1991-2000	12.6	-5.7	15.8	-3.2	56.1	-2.5	43.9
2001-2010	10.9	-7.4	16.7	-5.8	78.4	-1.6	21.6
1971-2010	12.3	-6.0	17.0	-4.7	78.3	-1.3	21.7



976  
977  
978  
979  
980  
981  
982  
983  
984  
985  
986

**Table 7** Changes of the inter-annual precipitation and temperature of the JRB.

Time	Precipitation (mm)	Temperature (°C)	$\Delta P$ (mm)	$\Delta T$ (°C)
1960s	561.2	8.6	—	—
1970s	500.1	8.8	-61.1	0.2
1980s	535.5	8.8	-25.6	0.2
1990s	462.4	9.4	-98.8	0.8
2000s	506.5	9.8	-54.6	1.2

Note:  $\Delta P$  and  $\Delta T$  are the changes in precipitation and temperature, respectively

987  
988  
989  
990  
991  
992  
993  
994  
995  
996  
997  
998  
999  
1000  
1001  
1002  
1003  
1004  
1005  
1006  
1007  
1008

1009  
1010  
1011  
1012  
1013  
1014  
1015  
1016

**Table 8** Cumulative area of soil and water conservation in the JRB at the end of different years  
(Unit:km<sup>2</sup>)

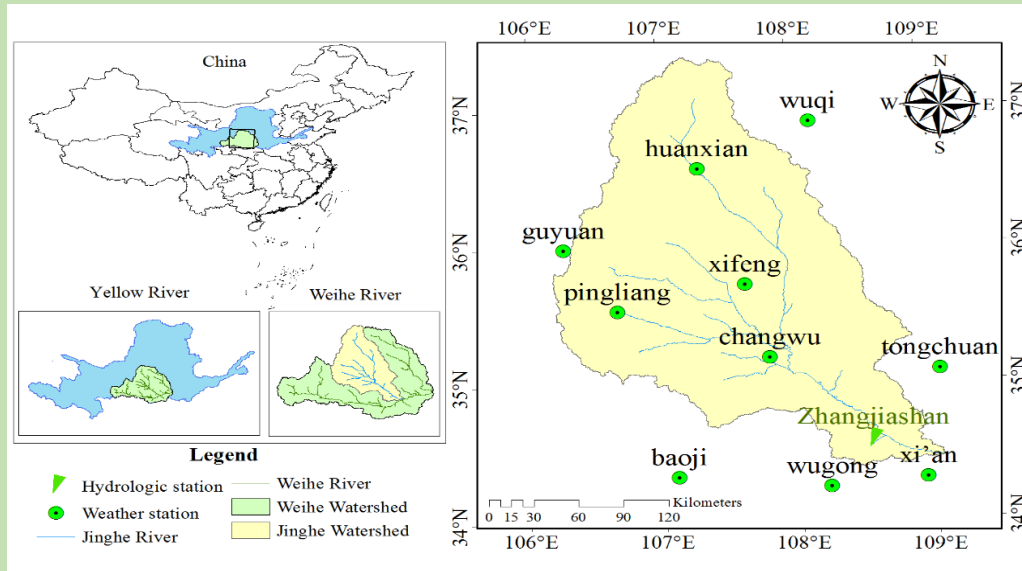
Time	Level terrace	Afforestation	Grass-planting	Check dam	Total
1960s	50	184	11	4	249
1970s	330	666	90	10	1096
1980s	729	1520	169	18	2436
1990s	2356	4135	1023	49	7563
2000s	2907	4773	1146	52	8878

1017  
1018  
1019  
1020  
1021  
1022  
1023  
1024  
1025  
1026  
1027  
1028  
1029  
1030  
1031

1032

1033

1034



1035

1036 **Figure 1.** Location of hydrological and meteorological stations along the Jinghe River.

1037

1038

1039

1040

1041

1042

1043

1044

1045

1046

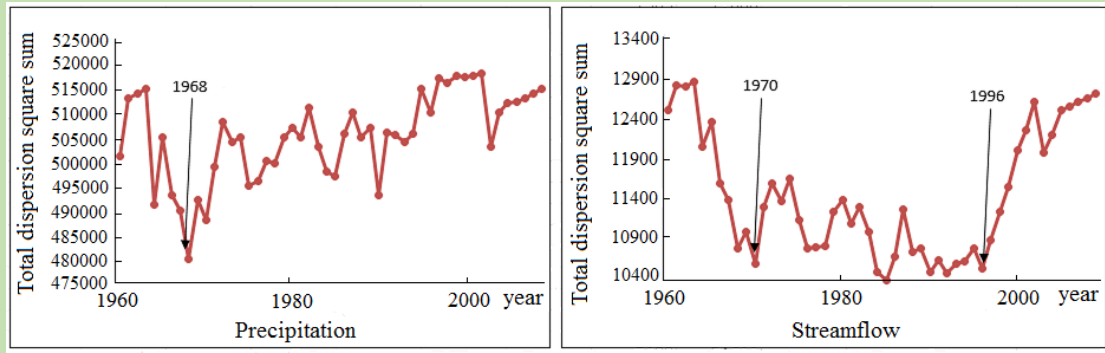
1047

1048

1049

1050

1051



1052

1053

**Figure 2.** The abrupt change points of precipitation and streamflow in the JRB with Sequential

1054

cluster.

1055

1056

1057

1058

1059

1060

1061

1062

1063

1064

1065

1066

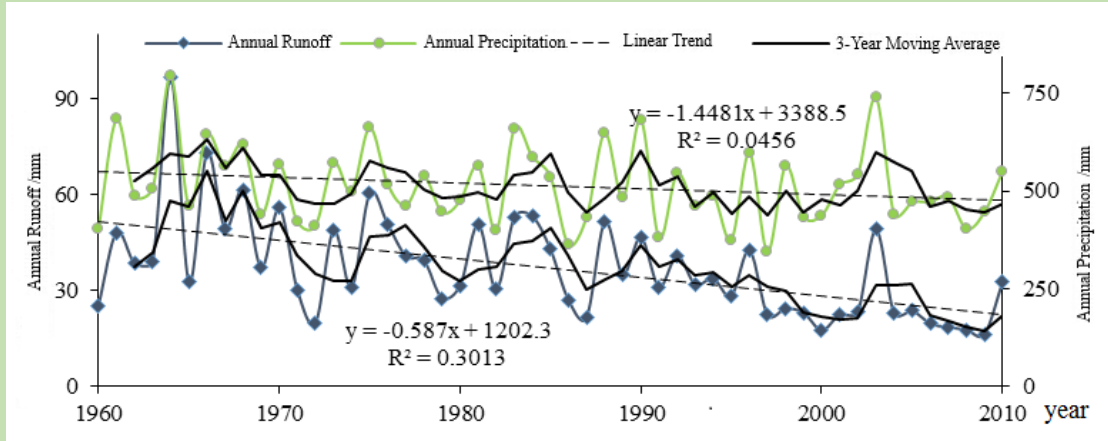
1067

1068

1069

1070

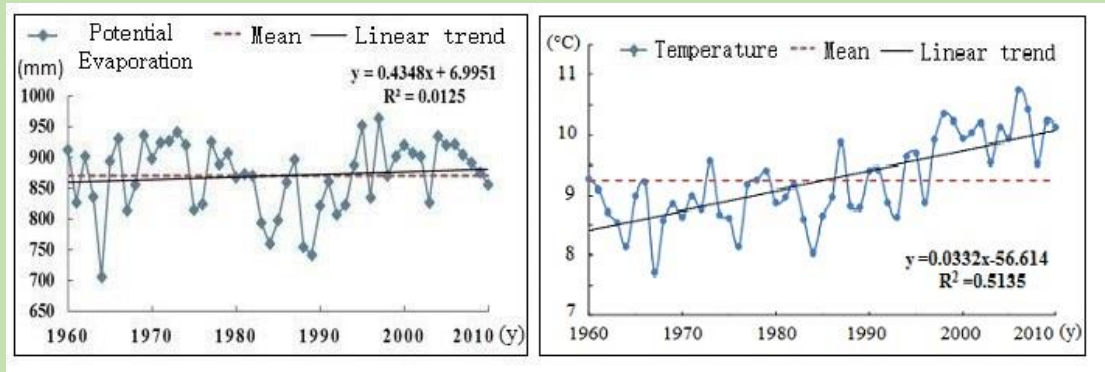
1071  
1072  
1073  
1074



1075  
1076  
1077  
1078  
1079  
1080  
1081  
1082  
1083  
1084  
1085  
1086  
1087  
1088  
1089  
1090  
1091  
1092  
1093  
1094

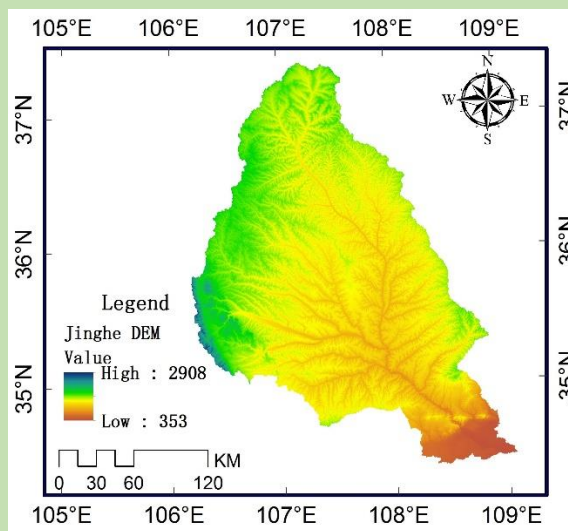
**Figure 3.** Changes of the annual streamflow and precipitation of the JRB.

1095  
1096  
1097  
1098  
1099

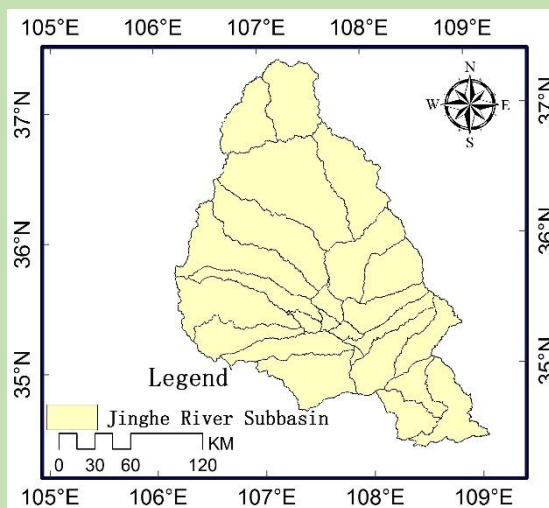


1100  
1101  
1102  
1103  
1104  
1105  
1106  
1107  
1108  
1109  
1110  
1111  
1112  
1113  
1114  
1115  
1116  
1117

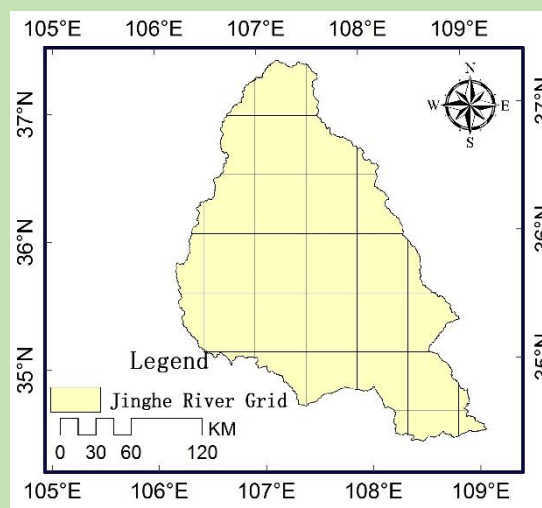
**Figure 4.** Changes of the annual potential evaporation and temperature of the JRB.



(a)



(b)



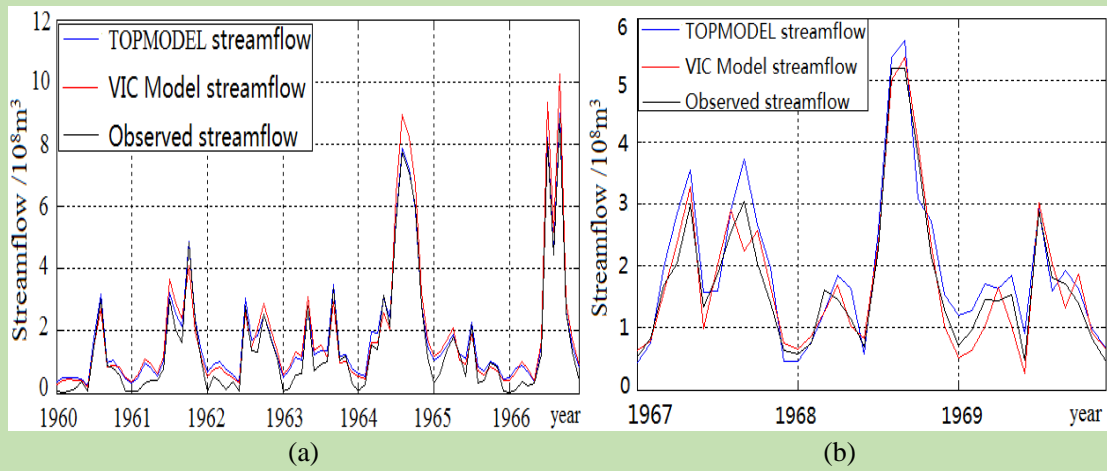
(c)

**Figure 5.** (a) Elevation maps of the study area at a 30-m resolution. (b) Sub-basin of TOPMODEL. (c) Grid of the VIC model.

1118  
1119

1120  
1121  
1122  
1123  
1124  
1125  
1126  
1127  
1128  
1129  
1130  
1131  
1132  
1133  
1134  
1135  
1136  
1137

1138  
1139  
1140



1141

1142

**Figure 6.** The simulated and observed streamflow for TOPMODEL and the VIC model.

1143

(a) Calibration period. (b) Validation period.

1144

1145

1146

1147

1148

1149

1150

1151

1152

1153

1154

1155

1156

1157

1158

1159

1160

1161

1162

1163

1164

1165

1166

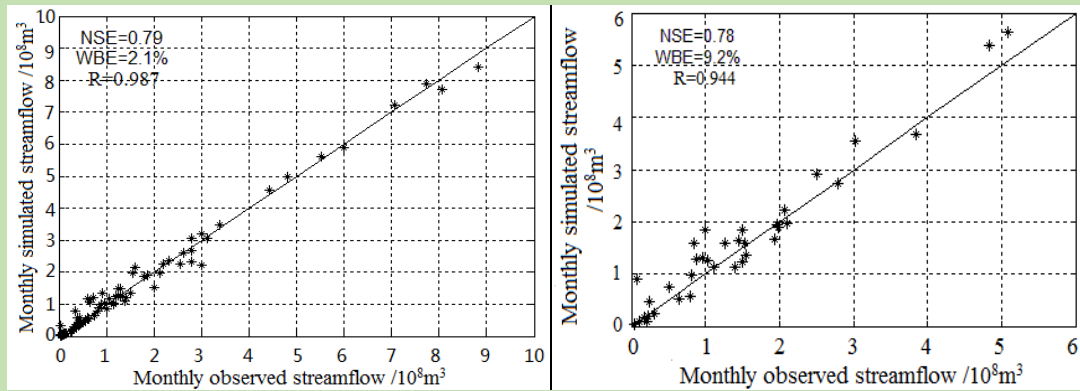
1167

1168

1169



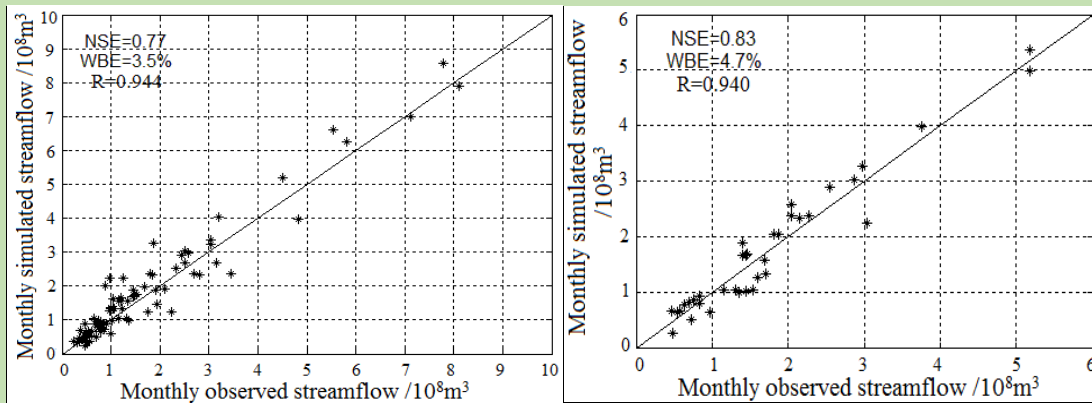
1170  
1171  
1172  
1173



1174  
1175  
1176

(a) Calibration streamflow for TOPMODEL

(b) Validation streamflow for TOPMODEL



1177  
1178

(c) Calibration streamflow for VIC model

(d) Validation streamflow for VIC model

1179

**Figure 7.** Comparison of the observed and modeled monthly streamflows for the calibration

1180

and validation periods.

1181

1182

1183

1184

1185

1186

1187

1188

1189

1190

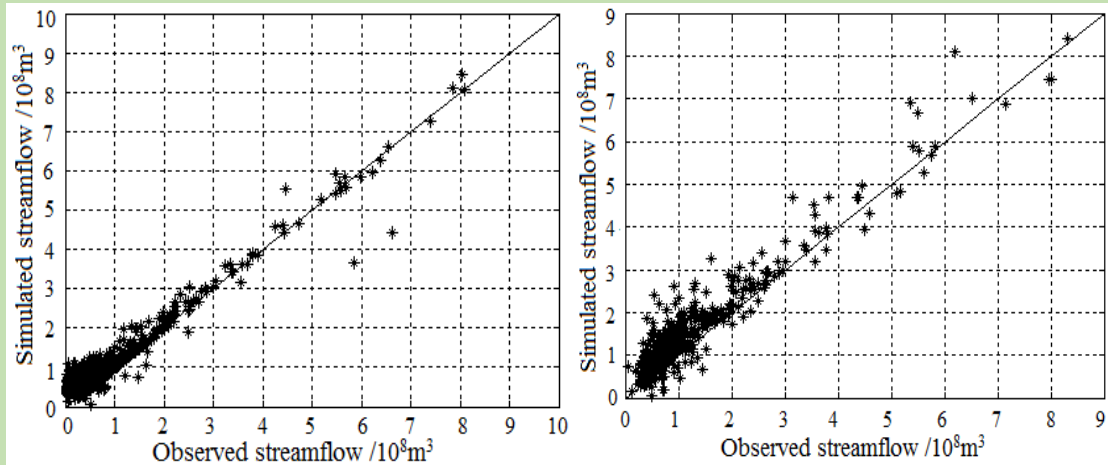
1191

1192

1193

1194

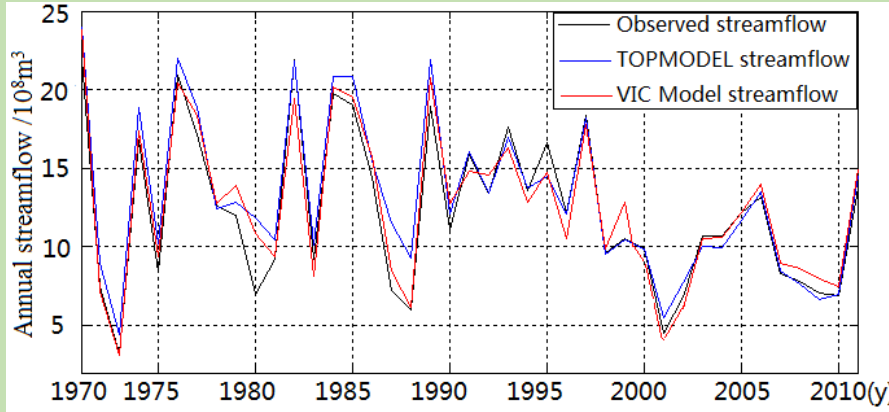
1195  
1196  
1197  
1198  
1199  
1200



1201  
1202  
1203  
1204  
1205  
1206  
1207  
1208  
1209  
1210  
1211  
1212  
1213  
1214  
1215  
1216  
1217  
1218  
1219  
1220  
1221  
1222  
1223  
1224  
1225  
1226  
1227

**Figure 8.** Comparison of the observed and modeled monthly streamflow in 1971-2010.  
(a)TOPMODEL. (b) VIC model.

1228  
1229  
1230  
1231  
1232  
1233



1234  
1235  
1236  
1237  
1238  
1239  
1240  
1241  
1242  
1243  
1244  
1245  
1246  
1247  
1248  
1249  
1250  
1251  
1252  
1253  
1254  
1255  
1256  
1257  
1258

**Figure 9.** Time series of the observed and modeled annual streamflow for the entire modeling period.